Heterozygous *MDR3* missense mutation associated with intrahepatic cholestasis of pregnancy: evidence for a defect in protein trafficking

P.H. Dixon[1,2,+], N. Weerasekera[1,2], K.J. Linton[2], O. Donaldson[1], J. Chambers[1], E. Egginton[3], J. Weaver[4], C. Nelson-Piercy[5], M. de Swiet[6], G. Warnes[2], E. Elias[3], C.F. Higgins[2], D.G. Johnston[1], M.I. McCarthy[1,2] and C. Williamson[1,26,§]

[1]Division of Medicine, Imperial College School of Medicine and [2]MRC Clinical Sciences Centre, Hammersmith Hospital, Du Cane Road, London W12 0NN, UK, [3]Department of Gastroenterology, Queen Elizabeth Hospital, Birmingham B15 2TH, UK, [4]Department of Obstetrics and Gynaecology, Birmingham Women's Hospital, Birmingham, B15 2TG, UK, [5]Department of Obstetrics, St Thomas' Hospital, Lambeth Palace Road, London SE1 7EH, UK and [6]Institute of Obstetrics and Gynaecology, Queen Charlottes' Hospital, Goldhawk Road, London W5 0XG, UK

Intrahepatic cholestasis of pregnancy (ICP) is a liver disease of pregnancy with serious consequences for the mother and fetus. Two pedigrees have been reported with ICP in the mothers of children with a subtype of autosomal recessive progressive familial intrahepatic cholestasis (PFIC) with raised serum γ-glutamyl transpeptidase (γ-GT). Affected children have homozygous mutations in the *MDR3* gene (also called *ABCB4*), and heterozygous mothers have ICP. More frequently, however, ICP occurs in women with no known family history of PFIC and the genetic basis of this disorder is unknown. We investigated eight women with ICP and raised serum γ-GT, but with no known family history of PFIC. DNA sequence analysis revealed a C to A transversion in codon 546 in exon 14 of *MDR3* in one patient, which results in the missense substitution of the wild-type alanine with an aspartic acid. We performed functional studies of this mutation introduced into *MDR1*, a closely related homologue of *MDR3*. Fluorescence activated cell sorting (FACS) and western analysis indicated that this missense mutation causes disruption of protein trafficking with a subsequent lack of functional protein at the cell surface. The demonstration of a heterozygous missense mutation in the *MDR3* gene in a patient with ICP with no known family history of PFIC, analysed by functional studies, is a novel finding. This shows that *MDR3* mutations are responsible for the additional phenotype of ICP in a subgroup of women with raised γ-GT.

INTRODUCTION

Intrahepatic cholestasis of pregnancy (ICP), also known as obstetric cholestasis, is a liver disorder of pregnancy with serious consequences for the mother and fetus (1–4). Cholestasis results from abnormal biliary transport from the liver into the small intestine, and ICP is characterized by the occurrence of cholestasis in pregnancy in women with an otherwise normal medical history. The classical maternal feature is generalized pruritus, becoming more severe with advancing gestation. ICP causes fetal distress, spontaneous premature delivery and unexplained third trimester intrauterine death (1–4). Delivery by 38 weeks gestation has reduced the perinatal mortality rate from 10–15% (1–2) to 2.0–3.5% (2–4). Abnormal maternal liver function tests (LFTs) are necessary to make the diagnosis. In particular, the serum total bile acid (BA) concentration is raised compared with normal pregnancy (5–8) and this is thought to be due to abnormal biliary transport across the hepatic canalicular membrane (9,10). All LFTs return to normal after delivery. In a subgroup of women the serum γ-glutamyl transpeptidase (γ-GT) level is also increased.

Several human autosomal recessive disorders are recognized to cause abnormal biliary transport. Progressive familial intrahepatic cholestasis (PFIC) is characterized by the onset of cholestasis in early childhood which can progress to cirrhosis and liver failure before adulthood (11), and can be classified into three subtypes (PFIC1–3). PFIC1 and 2 have low concentrations of biliary bile acids and low to normal γ-GT in the serum. PFIC1 (also called Byler disease) is clinically characterized by features of hepatic failure including jaundice, steatorrhoea and reduced growth, and is caused by mutations in the familial intrahepatic cholestasis 1 (*FIC1*) gene (12). Mutations in this gene have also been reported in benign recurrent intrahepatic cholestasis (BRIC), a separate condition in which affected individuals have

Table 1. Patient details

Patient no.	Parity[a]	Start of pruritus (gestational week)	Fetal distress[b]	Gestation at delivery (weeks + days)	Max. ALT[c] (<28 U/l)	Max. γ-GT[d] (<30 U/l)	Max. BA[e] (<6 mM)
1	1 + 0 (twins)	34	No	34 + 2	260	56	233
2	2 + 0	20	No	38	54	85	56
3	2 + 2	33	No	37 + 3	323	34	NT
4	4 + 4	36	Yes	38	163	36	45
5	3 + 4	31	Yes	36 + 2	691	74	34
6	1 + 0	32	No	36	NT	46	100
7	1 + 0	28	No	35 + 4	56[f]	134	236
8	2 + 2	15	Yes	35 + 6	163	50	237

NT not tested.
[a] Expressed as the number of live births + previous pregnancies that have not resulted in a live birth.
[b] Diagnosed if there was meconium staining of the amniotic fluid or fetal heart rate abnormality.
[c] Maximum alanine aminotransferase level (ALT). Normal range is given in parentheses.
[d] Maximum γ-glutamyl transpeptidase. Normal range is given in parentheses.
[e] Maximum bile acids (BA) level. Normal range is given in parentheses.
[f] Alanine aminotransferase level (ALT) was not available for patient 7, so the aspartate aminotransferase level (AST) is shown (normal range in the 3rd trimester <29 U/l).

transient episodes of cholestasis but do not develop hepatic failure (12). The *FIC1* gene encodes a P-type ATPase, which is believed to play a role in the enterohepatic circulation of bile acids. PFIC2 is caused by mutations in the bile salt export pump (*BSEP*) gene (13) (also called *ABCB11*). The clinical features of PFIC2 are similar to those of patients with PFIC1, although the appearance of the bile by electron microscopy is different (11), and the clinical outcome following orthotopic liver transplantation is better than for some PFIC1 patients (11,13).

PFIC3 patients are distinguished by high serum levels of γ-GT and bile which lacks phospholipid but has a normal biliary bile acid concentration (14), together with distinctive liver histology that shows portal duct inflammation and ductular proliferation (15). The raised serum γ-GT is a result of the detergent effect of the relatively high level of bile acid compared with phospholipid in the bile causing release of γ-GT from the biliary epithelium. Homozygous mutations of the multi-drug resistance 3 (*MDR3*) gene have been described in three pedigrees with PFIC3 (10,14). The heterozygote mothers of two affected children with PFIC3 had symptoms consistent with ICP (10,14). In one of these pedigrees in which a large consanguineous family had co-existing PFIC and ICP, three of the six mothers with ICP had pregnancies complicated by unexplained intrauterine death (10). Four of the six women were investigated and shown to be heterozygous for the *MDR3* mutation for which the proband was homozygous (10).

The *MDR3* gene [also known as *ABCB4* and *MDR2*, the homologue of murine *mdr2* (16,17)] encodes the MDR3 protein which is a member of the superfamily of ATP-binding cassette (ABC) transporters (18,19). The MDR3 protein has four domains: two homologous nucleotide-binding domains (NBDs) which bind and hydrolyse ATP and whose sequence is highly conserved throughout the ABC transporter family, and two hydrophobic transmembrane domains (TMDs) which span the membrane multiple times. The MDR3 protein has been shown to be localized to the hepatocyte canilicular membrane and demonstrated to be a phosphatidyl choline (PC) flippase (20–22).

It is possible that mutations of the *MDR3* gene cause the more prevalent disorder, ICP without a family history of PFIC.

We investigated this hypothesis by screening the *MDR3* gene in eight individuals with ICP and a raised γ-GT, but no known family history of PFIC. We describe here the identification of a heterozygote *MDR3* mutation in a patient with ICP. We report the functional characterization of the equivalent mutation in a closely related homologue of the gene (*MDR1*), which strongly suggests that the mutant membrane protein misfolds and fails to traffic properly from the endoplasmic reticulum (ER) to the cell membrane.
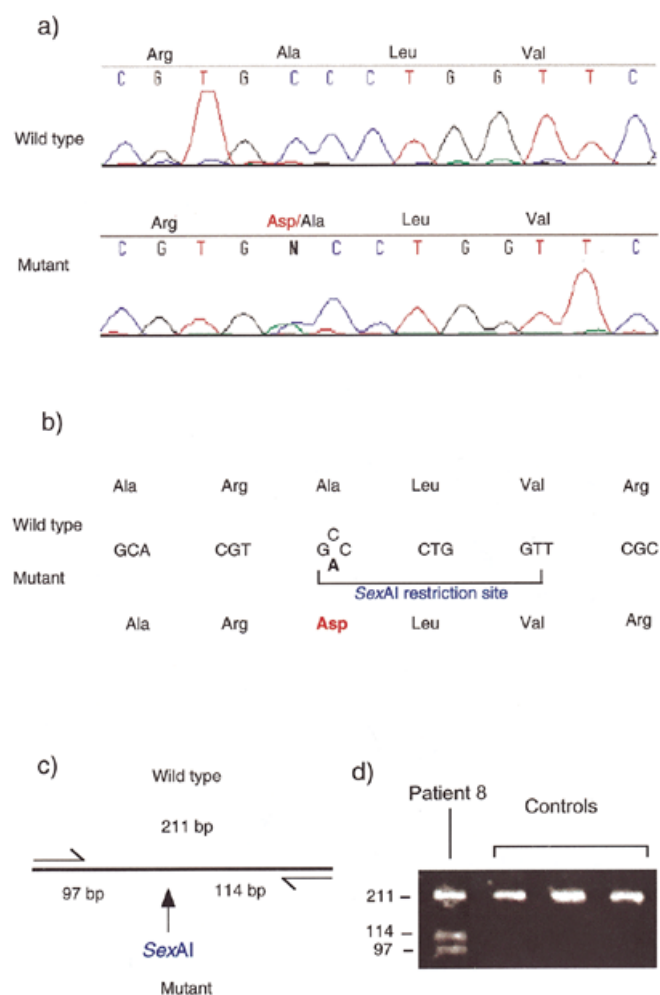
RESULTS

Mutation detection

DNA sequence analysis of the 27 coding exons of the *MDR3* gene, together with the respective exon–intron boundaries, was performed in eight ICP patients with raised γ-GT levels but no PFIC, together with a normal individual as a control. Patient details are given in Table 1.

In patient 8, a heterozygous DNA base change was identified in exon 14, at the second nucleotide of codon 546 (Fig. 1). In addition to the normal cytosine at this position, an adenine was also detected; this results in the substitution of the wild-type alanine with a mutant aspartic acid (A546D). This mutation is in the highly conserved first NBD of the MDR3 protein. The DNA base change introduces a *Sex*AI restriction enzyme site, which facilitated confirmation of the mutation (Fig. 1). This restriction enzyme change was used to exclude the presence of this mutation in two control panels consisting of 50 parous women without ICP and 40 ICP women without a known raised γ-GT during pregnancy. No other *MDR3* mutations were identified in the other seven individuals with ICP.

A546 is highly conserved in the NBDs of ABC transporters

A546 is a highly conserved residue, not only in the NBDs of proteins orthologous to the MDR3 protein in rat and mouse (16,23), but also in other members of the superfamily of ABC
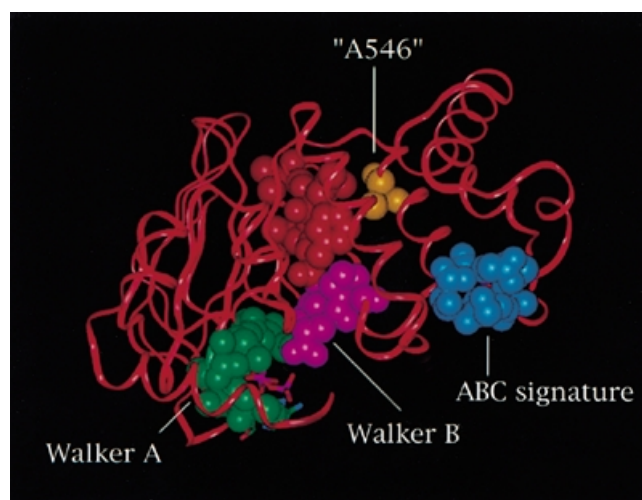
Figure 1. (**a**) The DNA sequence from patient 8 and a control patient. The C→A transversion results in the substitution of the wild-type alanine with an aspartic acid. The transversion also generates a *Sex*AI restriction site (**b**). Amplification of exon 14 by PCR gives a 211 bp product. If the C→A mutation is present, digestion of this product with *Sex*AI produces two smaller fragments of 97 and 114 bp, respectively (**c**). Thus, digestion of DNA from patient 8 with *Sex*AI reveals three products: the larger wild type product, and the two smaller fragments. In control subjects the 211 bp product is insensitive to cleavage by *Sex*AI (**d**).

Figure 2. Ribbon representation of the α-carbon backbone from the crystal structure of HisP (25), the NBD from the histidine permease of *Salmonella typhimurium*. The side chains of A167 (the equivalent of A546 in MDR3 protein), the Walker A motif, the Walker B motif and the ABC signature are shown space filled. The four hydrophobic residues at the N-terminal end of the Walker B motif are shown in red and the C-terminal residues are shown in purple. The bound ATP is shown as ball and stick.

transporters, including human P-glycoprotein (P-gp1) (24) and the NBD of the histidine permease (HisP) of *Salmonella typhimurium*. Whereas little is known about the structure of mammalian ABC transporters, the high resolution structure of HisP has been reported (25). From the crystal structure of HisP (25), A167 (the equivalent of the MDR3 protein A546) is located towards the C-terminus of α-helix 5 and, spatially, is in close proximity to the hydrophobic residues preceding the Walker B motif (Fig. 2).

Mature A544D-P-gp1 at the cell surface is functional

There are no established systems for quantification of PC translocation in mammalian systems making it currently not possible to study the function of the MDR3 protein. However, the transport of fluorescent substrates such as rhodamine by the multi-drug transporter P-gp1 is relatively easy to assay in mammalian cell culture systems. The MDR3 protein shares

77% identity with P-gp1 and it has been shown that substitution of as few as three adjacent MDR3 protein residues in the first TMD by the equivalent residues from P-gp1 is sufficient to allow the chimeric molecule to transport substrates specific to P-gp1 (26). The level of sequence identity between P-gp1 and the MDR3 protein increases to 87% in the NBDs. In addition, the NBDs of P-gp1 and the MDR3 protein have been shown to be interchangeable (27). We therefore introduced the equivalent A546D mutation into the first NBD of P-gp1 and studied the functional consequences of the change in transiently transfected mammalian cells.

Alignment of the amino acid sequence of human P-gp1 with the MDR3 protein identified A544 as the P-gp1 equivalent of MDR3 protein A546. Site-directed mutagenesis was used to alter codon 544 of *MDR1*, to encode an aspartic acid. The mutated fragment was subcloned into the plasmid pMDR1-wt to generate pMDR1-A544D, and used to transiently transfect human epithelial kidney (HEK293T) cells.

Fluorescence activated cell sorting (FACS) of live cells was used to correlate the ability of transiently transfected cells to extrude a fluorescent substrate of P-gp1, rhodamine 123 (R123). The presence of P-gp1 at the cell surface in the same batch of transfected cells was determined by the P-gp1-specific monoclonal antibody (mAb) UIC2 conjugated to phycoerythrin (UIC2-PE).

Cells transiently transfected with pCIneo-βgal which does not encode P-gp1 all behaved in a similar way and accumulated R123 and failed to label with UIC2-PE (Fig. 3a). In contrast, cells transiently transfected with pMDR1-A544D formed two distinct populations. The first population behaved similarly to the control cells with no UIC2-PE fluorescence and high R123 fluorescence (Fig. 3b, lower right quadrant), consistent with failure to express A544D-P-gp1 at the cell surface (and thus accumulate R123). The second cell population was characterized by high UIC2-PE fluorescence and no
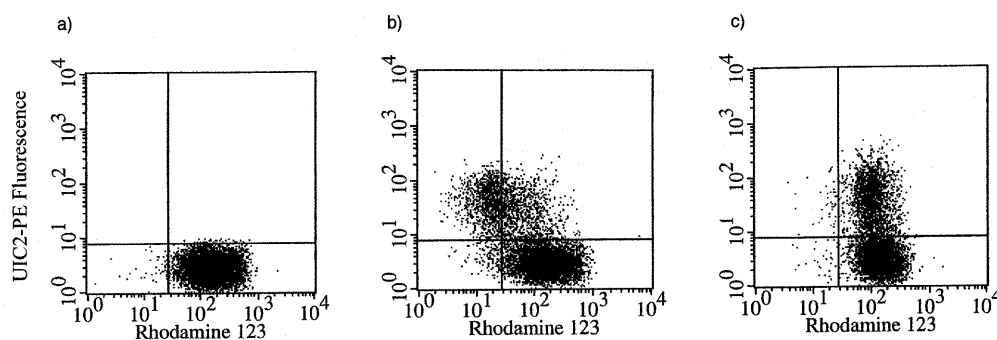
Figure 3. FACS analysis of HEK293T cells transiently transfected with pCIneo-βgal (**a**), or pMDR1-A544D (**b** and **c**). Cells were incubated first with the P-gp1 substrate R123 in the presence (**c**) or absence (**a** and **b**) of the P-gp inhibitor CsA. The cells were then incubated with the P-gp1-specific mAb (UIC2-PE) before FACS.

Table 2. Ratio of intracellular to cell surface P-glycoprotein

	Mean fluorescence (relative arbitrary fluorescence units)		
	A544D-P-gp1	Wt-P-gp1	HEK293T
Intact cells	40	171	3
F&P then labelled with UIC2-PE	197	497	13
Labelled with UIC2-PE then F&P	32	144	3
Intracellular P-gp	*155*	*343*	–
Cell surface P-gp	*37*	*168*	–
Total P-gp	*192*	*511*	–

Summary of the mean observed fluorescence of intact cells (Fig. 4), and of the mean fluorescence following fixation and permeabilization (F&P) either before or after P-gp1-specific mAb UIC2-PE labelling (Fig. 6). This allowed the intracellular, cell surface and total P-gp of wt-P-gp1 and A544D to be calculated (calculated values are shown in italics).

R123 fluorescence (Fig. 3b, upper left quadrant) consistent with cell surface expression of A544D-P-gp1 and extrusion of R123. Further confirmation that the extrusion of R123 in the A544D-P-gp1-expressing cells is due to the function of the mutant P-gp was obtained by incubating the cells with the P-gp1-inhibitor cyclosporin A. Under these conditions the cells with a high UIC2-PE fluorescence accumulated high levels of R123 fluorescence (Fig. 3c, upper right quadrant). These data are typical of cells expressing functional P-gp1 (28) and indicate that the A544D-P-gp1 mutant is functional if it reaches the cell membrane.

Evidence that A544D-P-gp1 is a trafficking mutant

The finding that substitution of an aspartic acid for an alanine in a highly conserved region of NBD1 did not alter the ability of the mature protein to transport R123 was unexpected and suggested that the equivalent A546D-MDR3 protein mutant would also be functional. However, the FACS analysis provided evidence that the mutant protein is inefficiently expressed compared with the wild-type protein (Table 2).
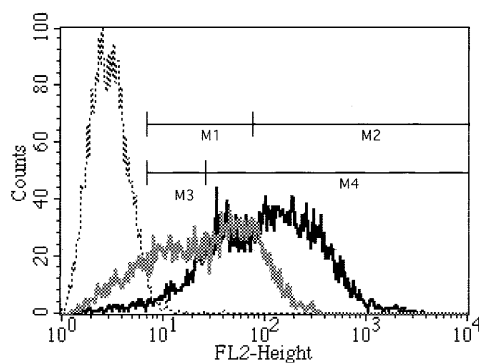
When transiently transfected with pMDR1-wt, 97% of HEK293T cells expressed wild-type P-gp1 at the cell surface [compare the UIC2-PE labelling of intact cells transfected with pCIneo-βgal or pMDR1-wt (Fig. 4)]. There were two populations of pMDR1-wt-transfected cells which differed by the amount of wild-type P-gp1 at the cell surface (Fig. 4). The first population (M1) had a mean UIC2-PE fluorescence of 38 rela-

tively arbitrary fluorescence units and the second population (M2) had a mean of 200. The overall mean fluorescence was 171, compared with a control value of 3. We suspect that those cells that have a lower level of P-gp1 at the cell surface (M1) took up the DNA shortly after mitosis and that this resulted in a lag phase of one cell cycle until the nuclear membrane dissolved to permit entry into the nucleus and expression of the *MDR1* gene. Effectively, these cells have had a delayed transfection time and so may have only had 24 h for gene expression from the introduced plasmid, which is insufficient time to accumulate maximal levels of wild-type P-gp1 at the cell surface. The population of cells that express high levels of P-gp1 at the cell surface (M2) probably entered mitosis soon after the introduction of the pMDR1-wt DNA and so have effectively had double the expression time.
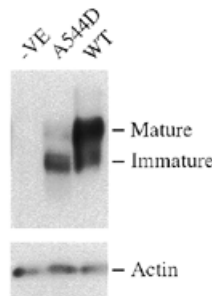
Cells transfected with pMDR1-A544D also formed two populations (Fig. 4); the first population (M3) had a mean UIC2-PE fluorescence of 10 [barely above the mean (= 3) of the negative control cells], and the second population (M4) had a mean of 50. The overall mean fluorescence was 40. These data indicate that the mutant protein is expressed at the cell surface at much lower levels than the wild-type protein (Table 2).

Western blot analysis of A544D-P-gp1

Transiently transfected cells normally express two forms of P-gp1, discernible by polyacrylamide gel electrophoresis (PAGE) and western analysis: immature, non- or core-glyco-

Figure 4. UIC2-PE antibody labelling of intact HEK293T cells transiently transfected with pCIneo-βgal (grey intermittent line), pMDR1-wt (black) or pMDR1-A544D (grey). The counts represent mean fluorescence (relative arbitrary fluorescence units), and this is summarised for intact cells in Table 2. The transfected populations were observed to consist of two separate populations (M1 and M2 for pMDR1-wt, M3 and M4 for pMDR1-A544D) with different amounts of protein at the cell surface.

Figure 5. Western analysis of HEK293T cells transiently transfected with pCIneo-βgal (–VE), pMDR1-A544D (A544D) and pMDR1-wt (WT). The blot was probed with anti-P-gp mAb, C219, and the 170 kDa mature, glycosylated form and the 140 kDa immature form of the protein are indicated. The blot was reprobed with anti-actin mAb to confirm that the same amount of protein (20 mg) was added to each lane.

sylated P-gp1 and mature glycosylated P-gp1. All of the immature P-gp1 is found in intracellular compartments (29), and probably represents nascent polypeptide in the ER. The glycosylation of the first extracellular loop of P-gp1 is completed in the distal cisternae of the Golgi apparatus. If the A544D mutation impairs the trafficking of the protein from the ER to the cell membrane then it might be expected to alter the ratio of immature to mature protein found in the cell. PAGE and western analysis (Fig. 5) showed that wild-type P-gp1 was expressed at higher levels than A544D-P-gp1 and was predominantly present as the 170 kDa mature, glycosylated form. In contrast, the A544D-P-gp1 was predominantly found in the 140 kDa immature form. Reprobing of the blot with anti-actin mAb indicated that the same amount of cell protein was added to each lane (Fig. 5).

The ratio of cell surface to intracellular P-gp1 is also altered in the A544D mutant

Additional evidence that A544D-P-gp1 is a trafficking mutant was provided by calculating the ratio of cell surface to intra-

cellular P-gp1 by FACS analysis (Fig. 6 and Table 2). Cells that were fixed with paraformaldehyde and permeabilized with saponin prior to incubation with antibody, provided an indication of the total P-gp in the cell (Fig. 6, black traces). The intracellular P-gp fraction was then determined by subtraction from this figure of the cell surface P-gp determined by incubation of live cells with antibody before fixation and permeabilization and FACS (Fig. 6, grey traces); this controlled for the possible loss of cell surface antibody–antigen conjugate during the fixation and permeabilization. It was also necessary to subtract the antibody bound non-specifically to cells as this fraction changes when intracellular antigens are exposed (Fig. 6c compare black and grey traces). These data, obtained for cells expressing wild-type P-gp1 and for cells expressing the A544D mutant, are summarized along with the background levels of fluorescence in Table 2. Calculation of total P-gp1 level and the ratio of intracellular to cell surface P-gp clearly showed that cells transfected with pMDR1-A544D expressed a lower level of P-gp1 than cells transfected with pMDR1-wt (total fluorescence 192 and 511, respectively), and that much less of it got to the cell surface (only 19% of the total produced, compared with 33% of wild-type protein). The western analysis of cells expressing wild-type P-gp1 demonstrated that there is more of the mature, glycosylated form than of the immature form of the protein. When considered together, these results demonstrate that not all of the mature protein is at the cell surface. These results show that the MDR3 mutation A546D causes abnormal protein glycosylation and trafficking when its equivalent is expressed in P-gp1.

DISCUSSION

Our analysis of the sequence of the coding region of the *MDR3* gene in eight patients with ICP and raised γ-GT has revealed the presence of a mutation in exon 14 (A546D) in one individual. This mutation was not found in 50 parous controls without ICP, nor in 40 ICP women without a raised γ-GT, indicating that it is not a common polymorphism. The location of this mutation within the highly conserved first NBD indicates that this is not likely to be a benign alteration, and we provide data showing that it interferes with protein trafficking. Thus, ICP without PFIC can be caused by mutations in *MDR3*. We only found a *MDR3* mutation in one of eight women; this could be because other mutations are in untranslated regions, or in regulatory regions of the gene that were not screened in this study.

To date, only three other mutations of the *MDR3* gene have been published, all in individuals with PFIC3 (10,14); in two of the pedigrees, the heterozygous mothers had symptoms consistent with ICP. These mutations are believed to cause loss of function, as they all introduce premature stop codons. The occurrence of the A546D mutation, the substitution of a hydrophobic amino acid with a charged polar amino acid, in the highly conserved first NBD, suggested that this mutation would also result in loss-of-function of the MDR3 protein. In order to gain insight into the functional consequences of this mutation, we tested the effects of the equivalent mutation to A546D in P-gp1 (A544D). Transient expression of A544D-P-gp1 in HEK293T cells, and subsequent FACS and western analysis suggested that this mutation reduces the abundance of the protein and impairs protein trafficking to the cell
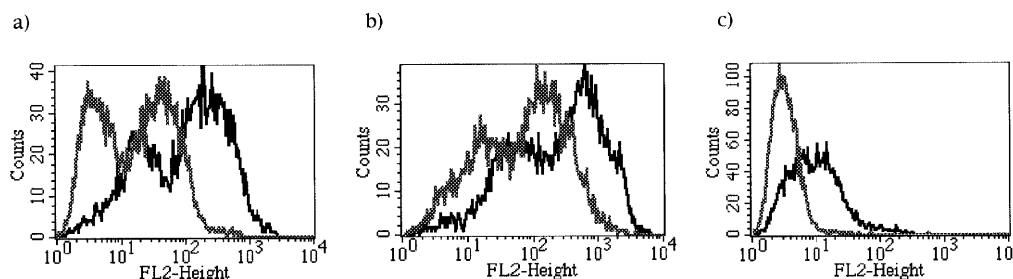
Figure 6. FACS analysis of cells transiently transfected with pMDR1-A544D (**a**), pMDR1-wt (**b**) or pCIneo-βgal (**c**). Fluorescence from cells which have been fixed with paraformaldehyde and permeabilized with saponin, prior to incubation with antibody (UIC2-PE) is shown in black, and from cells incubated with antibody before fixation and permeabilization in grey. The mean fluorescence for each population of cells is given in Table 2.

membrane. This probably arises as a consequence of misfolding of the first NBD leading to retention of the protein in the ER and an increase in the rate of degradation. The A546D mutation in the MDR3 protein is likely to have a similar phenotype as there is considerable sequence identity between the proteins in this domain (87%), and because the NBDs of P-gp1 and the MDR3 protein have been shown to be functionally interchangeable (27).

A number of missense mutations have been identified in other genes that result in trafficking defects, including the cystic fibrosis transmembrane conductance regulator (*CFTR*) gene (30,31), which encodes the CFTR protein, another member of the ABC transporter superfamily, and genes encoding the Wilson disease and Menkes disease proteins, both of which are P-type ATPases (32,33). Such mutations in membrane transport proteins commonly result in reduced function in addition to abnormal protein trafficking (32–34). However, a disease-causing mutation has been reported in *CFTR* which is associated with protein mislocalization, but normal CFTR protein function (31). The *MDR3* mutation we have identified may be similar, resulting in an increased proportion of mislocalized protein, but normal MDR3 protein function if it reaches the cell membrane. The results of our functional studies in P-gp1 support this hypothesis.

Western and FACS analysis suggest that cells transiently transfected with pMDR1-wt produce more of the mature, glycosylated form of wild-type P-gp1, but that the majority of this is not localized at the cell surface. There is *in vitro* evidence for the existence of cytoplasmic reservoirs of bile acid transporters in intracellular vesicles which are recruited to the hepatocyte canalicular membrane, resulting in increased bile acid transport (35). This mechanism has not been specifically investigated in P-gp1, but it is possible that mature P-gp1 also resides in the Golgi apparatus and recycles to the cell surface. It has also been demonstrated that the mature Wilson disease protein and the Menkes disease protein reside in the *trans*-Golgi apparatus and recycle to the cell surface when copper transport is required (32,33).

It is not known why women with ICP only develop symptoms of cholestasis in pregnancy. The short-term administration of oral oestrogens to women with a history of ICP causes pruritus and abnormal LFTs (36,37), suggesting that predisposed women develop ICP due to the cholestatic effect of raised oestrogens in pregnancy. Progestogens may also play a

role (6,38). Progestogens and oestrogens can inhibit MDR-catalysed drug efflux and interact with P-gp (39). It is therefore possible that raised serum oestrogens and progestogens in normal pregnancy cause reduced function of the MDR3 protein, and that women who are heterozygotes for a trafficking mutation in the MDR3 protein have a reduced ability to compensate for this.

Although the cause of fetal distress and intrauterine death in ICP is not fully understood, some studies have reported a more frequent occurrence of fetal distress in cases with high maternal (8) or fetal (40) bile acid levels. Loss of function of the MDR3 protein results in raised serum bile acids as a secondary effect, as is seen in children with PFIC3 (14) and the heterozygote mothers with ICP (10). Thus, *MDR3* mutations which result in raised serum bile acids, such as the one reported in this study, may predispose to fetal distress and subsequent unexplained intrauterine death.

Of the 87 patients with confirmed diagnosis of ICP and raised serum bile acids, 20 had a raised γ-GT. The finding that 23% of women with ICP had a raised γ-GT was of interest as the frequency of high γ-GT PFIC in non-consanguineous families is extremely low. However, there are several non-hereditary causes of cholestasis in pregnancy that can result in raised serum bile acids with a raised γ-GT, including viral hepatitis, autoimmune hepatitis, drug-induced cholestasis, cholelithiasis and other causes of biliary obstruction, e.g. malignancy. Although these diagnoses are rare and will have been excluded in the majority of women in this study, we did not have access to the results of these investigations in all of the women in whom the retrospective measurement of γ-GT was performed.

Therapeutic interventions to improve protein trafficking are under investigation for the ΔF508 mutation in CFTR (41), and this approach may be useful for the treatment of protein trafficking mutations in ICP.

In conclusion, we report a heterozygous missense mutation in the *MDR3* gene in a patient with ICP. Our analysis of this mutation in P-gp1 suggests that it results in abnormal protein trafficking and a subsequent lack of functional protein at the cell surface. These results confirm that *MDR3* mutations are responsible for ICP in some women with raised γ-GT. Identification and characterization of further mutations in this gene will greatly increase our understanding of the role of *MDR3* in this subgroup of women with ICP.

MATERIALS AND METHODS

Patients

For mutational analysis of the *MDR3* gene, eight patients with raised γ-GT were analysed together with a normal control individual. Of these eight individuals, two were recruited prospectively on detection of raised γ-GT and the remaining six were added following retrospective measurement of γ-GT levels from stored serum in 87 patients. Of the 87 patients with a confirmed diagnosis of ICP and raised serum bile acids, 20 had raised γ-GT. As different hospitals have different normal ranges for liver function tests, the upper end of the normal range in pregnancy was assumed to be 80% of the level quoted outside pregnancy for each hospital, consistent with published studies (42). Full clinical details of the patients are given in Table 1.

Having identified a mutation in patient 8, we had wanted to obtain blood samples from her relatives for DNA extraction to establish whether the mutation was maternally or paternally acquired, or sporadic. However, this was not possible because she was adopted and has no contact with her biological parents.

To check for the presence of sequence variants in normal individuals we utilized a panel of 50 women with gestational diabetes but with otherwise normal pregnancies who had no history of cholestasis. We also analysed 40 women with obstetric cholestasis without known raised γ-GT (the γ-GT was not tested in all cases).

Sequence analysis and mutation detection

Long-range PCR products covering parts of the *MRD3* gene were generated using primers designed from the published sequence (17). Products varying in size from 4 to 12.3 kb were amplified using the Expand long-range PCR kit (Boehringer Mannheim, East Sussex, UK), and subcloned using the TOPO XL kit (Invitrogen, Carlsbad, CA), according to the manufacturer's instructions. Multiple independent positive colonies were picked and DNA prepared using the Wizard miniprep kit (Promega, Maddison, WI). Inserts were sequenced with vector-specific and *MDR3*-specific primers using the FS+ Dye Terminator sequencing kit (PE Applied Biosystems, Foster City, CA) according to the manufacturer's instructions. Products were resolved and the sequence determined using a 373XL semi-automated sequencer (PE Applied Biosystems), and the sequence analysed utilising the Sequence Analysis, Sequence Navigator and AutoAssembler software packages (PE Applied Biosystems).

Sequence information from these experiments was combined with previously published information (17) and with sequence information from the Washington University chromosome 7 sequencing project (http://genome.wustl.edu/gsc) to design 27 pairs of exon-specific primers for the *MDR3* gene (available from the authors on request). These primers were utilized to amplify the 27 coding exons of the *MDR3* gene together with the respective exon–intron boundaries. Amplification of genomic DNA by PCR was carried out using an automated DNA thermal cycler (MJ Research Tetrad, Genetics Research Instrumentation Ltd, Felstead, Essex) in a total volume of 50 µl containing 50–100 ng of DNA template, 100 ng of each oligonucleotide primer, 50 mM KCl, 10 mM Tris–HCl pH 8.3, 1–3 mM $MgCl_2$, 0.01% gelatin, 100 mM dNTP and 2 U *Taq* polymerase (Bioline,

London, UK). Reaction conditions were as follows: 96°C for 3 min, 35 cycles of 30 s at 94°C, 30 s at 55–62°C and 1 min at 72°C, followed by a final extension for 10 min at 72°C. Following amplification, products were gel-purified and subject to DNA sequencing reactions as described above to obtain sequence for both strands of the PCR product. Sequences were compared with the Sequence Navigator software package (PE Applied Biosystems).

Digestion of the PCR products with the restriction enzyme *Sex*AI (New England Biolabs, Beverley, MA), to assay for the presence of the mutated sequence, was carried out in a 30 µl volume using the conditions recommended by the manufacturer. Restriction fragments were resolved on 2% agarose gels.

Study of the MDR3 protein A546D mutation in P-gp1

Plasmid pMDR-wt encodes wild-type P-gp1 with a hexa-histidine tag at the C-terminus and has been described previously (28). This protein shows normal P-gp1 activity. Plasmid pCIK-βgal was kindly provided by D. Gill, University of Oxford, UK, and is based on pCI (Promega) which was engineered to express the *lacZ* sequence. Plasmid pSBH is based on the mutagenesis vector pAlter (Promega) and contains the first half of wild-type *MDR1* from the *Bam*HI site 5′ to the coding sequence, to the *Hin*dIII site spanning codons 681 and 682.

Site-directed mutagenesis

Alignment of the amino acid sequence of human P-gp1 with the MDR3 protein identified A544 as the P-gp1 equivalent of MDR3 protein A546. Site-directed mutagenesis was used to alter codon 544 of *MDR1* to encode an aspartic acid, adopting the C→A tranversion of the second position of the codon analogous to the A546D mutant of the MDR3 protein. The A544D mutation was introduced into NBD1 of P-gp1 by oligonucleotide-directed mutagenesis ('Altered sites' II; Promega) of pSBH. The mutagenic oligonucleotide (5′-CGCCATTGCAC-GAGACCTGGTTCGCAAC-3′) introduced the desired codon change at the same time as removing the adjacent *Pml*I restriction site without further alteration to the amino acid sequence of P-gp1. The nucleotide sequence of the mutated DNA was verified by automated DNA sequencing as described above, prior to subcloning the mutated *Eco*RI–*Hin*dIII DNA fragment back into pMDR-wt to generate pMDR-A544D.

A further change, thymine (T) to adenine (A) was made in the wobble position of codon 543 of *MDR1* to remove, silently, the *Pml*I restriction site in order to follow the subsequent subcloning events. The mutated fragment was subcloned into pMDR1-wt to generate pMDR1-A544D for expression studies in mammalian cells.

Transient transfection of mammalian HEK293T cells

HEK293T human epithelial kidney cells (3.75×10^6; Imperial Cancer Research Fund, cell production unit, Clare Hall, London, UK) were seeded on to a 75 cm^2 tissue culture flask in 15 ml of Dulbecco's modified Eagle's medium (DMEM), supplemented with 2 mM L-glutamine and 10% (v/v) fetal calf serum (FCS; Helena Biosciences, Sunderland, UK). The cells were incubated under 5% CO_2 at 37°C for 18 h to give ~70% confluency at which point the cells were transfected with polyethyleneimine (PEI)–DNA complexes: 60 µg of DNA in 30 µl

5% glucose was mixed with 9 µl of 25 kDa PEI solution [45mg PEI (Sigma Aldrich, Gillingham, UK) dissolved in 8 ml H_2O, corrected to pH 7.2 with dilute HCl]; this was diluted in 10 ml of supplemented DMEM and added directly to the cell monolayer. Twenty-four hours post-transfection the medium was replaced with fresh DMEM plus 2 mM butyric acid (Sigma Aldrich) to enhance expression of P-gp. The cells were harvested a further 24 h later.

Western analysis

Whole cell lysates were prepared from 5×10^5 transiently transfected cells by resuspension of the washed cell pellet in 300 µl lysis buffer [phosphate-buffered saline (PBS; pH 7.4), 1% SDS, 100 µM phenylmethylsulfonyl fluoride, 1 mM benzamidine, 4 µg/ml pepstatin and 1 mM ethylenediaminetetraacetic acid]. Cell lysate (10 µg) was separated by SDS–PAGE and the proteins transferred electrophoretically to PVDF membrane (Immobilon-P; Millipore, Bedford, MA). The membrane was probed with the anti-P-gp monoclonal antibody, C219 (Cis-Bio International, Gif-sur-Yvette, France), and developed using horseradish peroxidase-conjugated goat anti-mouse antibody and enhanced chemiluminescence (Amersham, Uppsala, Sweden).

FACS analysis

Dual labelling of intact cells was used to assay for both P-gp function and localization at the cell membrane. Transiently transfected HEK293T (1.25×10^6) cells were harvested by incubation with versene (2 mM EDTA in PBS) for 10 min at 37°C. The cells were washed twice with PBS and then incubated with 2 µM rhodamine 123 (R123; Sigma Aldrich), with or without cyclosporin A (CsA; 10 µM), and incubated for a further 30 min at 37°C. The cells were washed three times with versene, then incubated with 20 µg/ml anti-P-gp antibody [UIC2, phycoerythrin conjugate (UIC2-PE); Immunotech, Marseille, France] or isotype control diluted in FACS buffer (1% FCS in PBS) for 15 min at 4°C. The cells were washed three times in FACS buffer before resuspension in 300 µl of FACS buffer. Samples were stored in the dark at 4°C until analysis. Flow cytometric analysis of the cells (10 000) was carried out using a FACS Vantage flow cytometer (Becton Dickinson, San Diego, CA) fitted with an argon ion laser. PE fluorescence was measured at 575 nm and R123 fluorescence at 515 nm. Fluorescence data was analysed using CELLQuest (Becton Dickinson) software.

To detect intracellular antigen, 1.25×10^6 cells, harvested and washed as before, were fixed by addition of formaldehyde to 3% and incubated at room temperature for 20 min. The cells were washed three times in FACS buffer and resuspended in 0.5% saponin (in FACS buffer) and incubated for 20 min at 4°C. The cells were washed a further three times in FACS buffer before incubation with UIC2 and FACS as before.

ACKNOWLEDGEMENTS

REFERENCES

1. Reid, R., Ivey, K.J., Rencoret, R.H. and Storey, B. (1976) Fetal complications of obstetric cholestasis. *Br. Med. J.*, **1**, 870–872.
2. Reyes, H. (1982) The enigma of intrahepatic cholestasis of pregnancy: lessons from Chile. *Hepatology*, **2**, 87–96.
3. Fisk, N.M. and Storey, G.N.B. (1988) Fetal outcome in obstetric cholestasis. *Br. J. Obstet. Gynecol.*, **95**, 1137–1143.
4. Rioseco, A.J., Ivankovic, M.B., Manzur, A., Hamed, F., Kato, S.R., Parer, J.T. and Germain, A.M. (1994) Intrahepatic cholestasis of pregnancy: a retrospective case–control study of perinatal outcome. *Am. J. Obstet. Gynecol.*, **170**, 890–895.
5. Sjovall, K. and Sjovall, J. (1966) Serum bile acid levels in pregnancy with pruritus. *Clin. Chem. Acta*, **13**, 207–211.
6. Bacq, Y., Myara, A., Brechot, M.C., Hamon, C., Studer, E., Trivin, F. and Metman, E.H. (1995) Serum conjugated bile acid profile during intrahepatic cholestasis of pregnancy. *J. Hepatol.*, **22**, 66–70.
7. Laatikainen, T.J. and Ikonen, E. (1977) Serum bile acids in cholestasis of pregnancy. *Obstet. Gynecol.*, **50**, 313–318.
8. Laatikainen, T.J. and Tulenheimo, A. (1984) Maternal serum bile acid levels and fetal distress in cholestasis of pregnancy. *Int. J. Gynaecol. Obstet.*, **22**, 91–94.
9. Meng, L.J., Reyes, H., Palma, J., Hernandez, I., Ribalta, J. and Sjovall, J. (1997) Profiles of bile acids and progesterone metabolites in the urine and serum of women with intrahepatic cholestasis of pregnancy. *J. Hepatol.*, **27**, 346–357.
10. Jacquemin, E., Crestil, D., Manouvier, S., Boute, O. and Hadchouel, M. (1999) Heterozygous nonsense mutation in the MDR3 gene in familial intrahepatic cholestasis of pregnancy. *Lancet*, **353**, 210–211
11. Bull, L.N., Carlton, V.E., Stricker, N.L., Baharloo, S., DeYoung, J.A., Freimer, N.B., Magid, M.S., Kahn, E., Markowitz, J., DiCarlo, F.J. *et al.* (1997) Genetic and morphological findings in progressive familial intrahepatic cholestasis (Byler disease [PFIC-1] and Byler syndrome): evidence for heterogeneity. *Hepatology*, **26**, 155–164.
12. Bull, L.N., van Eijk, M.J.T., Pawlikowska, L., DeYoung, J.A., Juijn, J.A., Liao, M., Klomp, L.W.J., Lomri, N., Berger, R., Scharschmidt, B.F. *et al.* (1998) A gene encoding P-type ATPase mutated in two forms of hereditary cholestasis. *Nature Genet.*, **18**, 219–224.
13. Strautnieks, S.S., Bull, L.N., Knisely, A.S., Kocoshis, S.A., Dahl, N., Arnell, H., Sokal, E., Dahan, K., Childs, S., Ling, V. *et al.* (1998) A gene encoding a liver-specific ABC transporter is mutated in progressive familial intrahepatic cholestasis. *Nature Genet.*, **20**, 233–238.
14. de Vree, J.M.L., Jacquemin, E., Sturm, E., Cresteil, D., Bosma, P.J., Aten, J., Deleuze, J.-F., Desrochers, M., Burdelski, M., Bernard, O. *et al.* (1998) Mutations in the *MDR3* gene cause progressive familial intrahepatic cholestasis. *Proc. Natl Acad. Sci. USA*, **95**, 282–287.
15. Maggiore, G., Bernard, O., Riely, C.A., Hadchouel, M., Lemonnier, A. and Alagille, D. (1991) Diagnostic value of serum gamma-glutamyl transpeptidase activity in liver diseases in children. *J. Pediatr. Gastroenterol. Nutr.*, **12**, 21–26.
16. Gros, P., Ben Neriah, Y.B., Croop, J.M. and Housman, D.E. (1986) Isolation and expression of a complementary DNA that confers multidrug resistance. *Nature*, **323**, 728–731.
17. Linke, C.R., Smit, J.J.M., van der Velde-Koerts, T. and Borst, P. (1991) Structure of the human MDR3 gene and physical mapping of the human MDR3 locus. *J. Biol. Chem.*, **266**, 5303–5310.
18. Higgins, C.F., Hiles, I.D., Salmond, G.P., Gill, D.R., Downie, J.A., Evans, I.J., Holland, I.B., Gray, L., Buckel, S.D., Bell, A.W. *et al.* (1986) A family of related ATP-binding subunits coupled to many distinct biological processes in bacteria. *Nature*, **323**, 448–450.
19. Higgins, C.F. (1992) ABC transporters: from microorganisms to man. *Annu. Rev. Cell. Biol.*, **6**, 67–113.
20. Ruetz, S. and Gros, P. (1994) Phosphatidylcholine translocase: a physiological role for the mdr2 gene. *Cell*, **77**, 1071–1081.
21. Smith, A.J., Timmermans-Hereijgers, J.L., Roelofsen, B., Wirtz, K.W., van Blitterswijk, W.J., Smit, J.J., Schinkel, A.H. and Borst, P. (1994) The human MDR3 P-glycoprotein promotes translocation of phosphatidylcholine through the plasma membrane of fibroblasts from transgenic mice. *FEBS Lett.*, **354**, 263–266.
22. van Helvoort, A., Smith, A.J., Sprong, H., Fritzsche, I., Schinkel, A.H., Borst, P. and van Meer, G. (1996) MDR1 P-glycoprotein is a lipid translocase of broad specificity, while MDR3 P-glycoprotein specifically translocates phosphatidylcholine. *Cell*, **87**, 507–517.

23. Brown, P.C., Thorgeirsson, S.S. and Silverman, J.A. (1993) Cloning and regulation of the rat mdr2 gene. *Nucleic Acids Res.*, **21**, 3885–3891.

24. Chen, C., Chin, J.E., Ueda, K., Clark, D.P., Pastan, I., Gottesman, M.M. and Roninson, I.B. (1986) Internal duplication and homology with bacterial transport proteins in the mdr1/P-glycoprotein gene from multidrug resistant human cells. *Cell*, **47**, 381–389.

25. Hung, L.-W., Wang, I.X., Nikaido, K., Liu, P.-Q., Ames, G.F.-L. and Kim, S.-H. (1998) Crystal structure of the ATP-binding subunit of an ABC transporter. *Nature*, **396**, 703–707.

26. Zhou, Y., Gottesman, M.M. and Pastan, I. (1999) Studies of human MDR1-MDR2 chimeras demonstrate the functional exchangeability of a major transmembrane segment of the multidrug transporter and phosphatidylcholine flippase. *Mol. Cell. Biol.*, **19**, 1450–1459.

27. Buschman, E. and Gros, P. (1991) Functional analysis of chimeric genes obtained by exchanging homologous domains of the mouse mdr1 and mdr2 genes. *Mol. Cell. Biol.*, **11**, 595–603.

28. Blott, E.J., Higgins, C.F. and Linton, K.J. (1999) Cysteine scanning mutagenesis provides no evidence for the extracellular accessibility of the nucleotide-binding domains of the multidrug resistance transporter P-glycoprotein. *EMBO J.*, **18**, 6800–6808.

29. Loo T.W. and Clarke, D.M. (1995) Membrane topology of a cysteine-less mutant of human P-glycoprotein. *J. Biol. Chem.*, **270**, 838–848.

30. Cheng, S.H., Gregory, R.J., Marshall, J., Paul, S., Souza, D.W., White, G.A., O'Riordan, C.R. and Smith, A.E. (1990) Defective intracellular transport and processing of CFTR is the molecular basis of most cystic fibrosis. *Cell*, **63**, 827–834.

31. Smit, L.S., Strong, T.V., Wilkinson, D.J., Macek Jnr, M., Mansoura, M.K., Wood, D.L., Cole, J.L., Cutting, G.R., Cohn, J.A., Dawson, D.C. *et al.* (1995) Missense mutation (G480C) in the CFTR gene associated with protein mislocalisation but normal chloride channel activity. *Hum. Mol. Genet.*, **4**, 269–273.

32. Ambrosini, L. and Mercer, J.F.B. (1999) Defective copper-induced trafficking and localization of the Menkes protein in patients with mild and copper-treated classical Menkes disease. *Hum. Mol. Genet.*, **8**, 1547–1555.

33. Payne, A.S., Kelly, E.J. and Gitlin, J.D. (1998) Functional expression of the Wilson disease protein reveals mislocalisation and impaired copper-dependent trafficking of the common H1069Q mutation. *Proc. Natl Acad. Sci. USA*, **95**, 10854–10859.

34. Drumm, M.L., Wilkinson, D.J., Smit, L.S., Worrell, R.T., Strong, T.V., Frizzell, R.A., Dawson, D.C. and Collins, F.S. (1991) Chloride conductance expressed by delta F508 and other mutant CFTRs in Xenopus oocytes. *Science*, **254**, 1797–1799.

35. Boyer, J.L. and Soroka, C.J. (1995) Vesicle targeting to the apical domain regulates bile excretory function in isolated rat hepatocyte couplets. *Gastroenterology*, **109**, 1600–1611.

36. Kreek, M.J., Weser, E., Sleisenger, M.H. and Jeffries, G.H. (1967) Idiopathic cholestasis of pregnancy: the response to challenge with the synthetic estrogen, ethinyl estradiol. *N. Engl. J. Med.*, **277**, 1391–1395.

37. Holzbach, R.T., Sivak, D.A. and Braun, W.E. (1983) Familial recurrent intrahepatic cholestasis of pregnancy: a genetic study providing evidence for transmission of a sex-limited, dominant trait. *Gastroenterology*, **85**, 175–179.

38. Bacq, Y., Sapey, T., Brechot, M.C., Pierre, F., Fignon, A. and Dubois, F. (1997) Intrahepatic cholestasis of pregnancy: a French prospective study. *Hepatology*, **26**, 358–364.

39. Taylor, J.C., Ferry, D.R., Higgins, C.F. and Callaghan, R. (1999) The equilibrium and kinetic drug binding properties of the mouse P-gp1a and P-gp1b P-glycoproteins are similar. *Br. J. Cancer*, **81**, 783–789.

40. Laatikainen, T.J. (1975) Fetal bile acid levels in pregnancies complicated by maternal intrahepatic cholestasis. *Am. J. Obstet. Gynecol.*, **122**, 852–856.

41. Brown, C.R., Hong-Brown, L.Q., and Welch, W.J. (1997) Strategies for correcting the delta F508 CFTR protein-folding defect. *J. Bioenerg. Biomembr.*, **29**, 491–502.

42. Girling, J.C., Dow, E. and Smith, J.H. (1997) Liver function tests in pre-eclampsia: importance of comparison with a reference range derived for normal pregnancy. *Br. J. Obstet. Gynecol,* **104**, 246–250.